Electronic Supplementary Material (ESI) for Journal of Materials Chemistry A.

Supplementary data

Three-dimensional hierarchical MoO_2/MoC@NC-CC free-standing anode applied in microbial fuel cells

Da Liu,[a] Wenkai Fang,[a] Jiangtao Li,[a] Liling Zhang,[a] Mei Yan,[b*] and Hongwu Tang,[a*]

a. *College of Chemistry and Molecular Sciences, Wuhan University, Wuhan 430072, China*

b. *School of Chemistry and Chemical Engineering, Harbin Institute of Technology, Harbin 150001, China*

* Corresponding authors. E-mail addresses: yanmei@hit.edu.cn (M. Yan), hwtang@whu.edu.cn (H. W. Tang)

2. Materials and methods

2.1 Synthesis of MoO_2/MoC@NC-CC electrodes

Mo-precursor nanodendrites-CC was first prepared by a simple solvothermal reaction [S1]. Briefly, 0.266 g of ammonium molybdate was dispersed in 16 mL of *N, N*-dimethylformamide under magnetic stirring for 10 min to obtain a homogeneous solution. Then, the above solution was transferred to a 40 mL Teflon-lined stainless autoclave at 200 ℃ for 15 h and the carbon cloth (1×3 cm) was immersed vertically in this solution. After the autoclave cooled naturally, the Mo-precursor-CC was rinsed with absolute ethanol and dried at 60 ℃ in air. Subsequently, the MoC-CC was fabricated by carbonization at 750 ℃ for 2 h under a flow of N_2 with a heating rate of 10℃ min^{-1}, accompanied by Mo-precursor-CC and 0.5 g of DCDA (at the upstream side) placed in tube furnace. Third, the MoC@PANI core/shell arrays were prepared by a simple electro-deposition (ED) method. The MoC nanodendrites arrays serve as the backbone for the growth of PANI shell. The ED was conducted in three-electrode system with electrolyte of 1.5 mL aniline, 1.5 mL sulfuric acid and 150 mL distilled water by applying constant anodic current density of 2.5 mA cm^{-2} for 900 s. The MoC-CC was used as the working electrode, Ag/AgCl as the reference electrode and a Pt foil as the counter electrode. Finally, the MoO_2/MoC@NC-CC was obtained via carbonizing MoC@PANI-CC in a quartz furnace at 750 ℃ for 2 h under N_2 atmosphere with a heating rate of 5 ℃ min^{-1}

2.2 Characterization

XRD patterns were detected by Powder X-ray diffraction (XRD) with Cu Kα radiation (λ = 0.154 nm) at 40 KV and 40 mA (D8 Advance, Bruker). The morphology and microstructure were performed on Field Emission Scanning Electron Microscope (FESEM, Zeiss SIGMA, Carl Zeiss) and Transmission Electron Microscope (TEM, JEM-2100, JEOL). The chemical composition of the electrode surface was carried out by X-ray photoelectron spectroscopic (XPS) using a ESCALAB 250Xi instrument (Thermo

Fisher Scientific, USA). The hydrophilic property of the electrodes surface was characterized by the contact angle tester (DSA100S, KRUSS, Germany).

Electrochemical measurements were conducted with an electrochemical workstation (DH7000, Donghua Analytical Instruments Co., Ltd, China) in a standard three-electrode system using Pt foil as the counter electrode, and an Ag/AgCl electrode (KCl saturated) as the reference electrode. Before inoculation, Cyclic voltammetry (CV) was measured in fresh anolyte (Fig. 3a) from -0.8 to 0.2 V with a scan rate of 5 mV s^{-1}. After biofilm formation, CV and differential pulse voltammetry (DPV) were tested under turnover condition (the output voltages at the plateau). Electrochemical impedance spectroscopy (EIS) of the abiotic electrode and bioanode was carried out in 50 mM phosphate buffer solution (PBS) containing 5 mM potassium ferricyanide with the following parameters: the frequency range: 0.01Hz ~ 100 kHz, direct current potential: 0.2 V, amplitude:10 mV. For specific area capacitance, it is calculated from the CV curves (Fig.3a) according to Eq. (1):

$$Ca = A/(2 \cdot \Delta V \cdot S \cdot v) \quad (1)$$

Where, Ca is specific areal capacitance (mF/cm^2); A is the absolute integral area of the CV curve; ΔV is the potential range (V); S is the surface area of the electrode (cm^2); and *v* is the scan rate (mV/s) [S2].

For the determination of bioanode microbial community, DNA extraction was performed after 30 d steady and repeatable voltage output. The anode was taken out and cut into small pieces to extract the bacterial DNA using SPINeasy DNA Kit for soil according to the manufacturer's protocol. The DNA concentration was analyzed by a spectrophotometer (NanoDrop 2000c, Thermo Fisher, USA). For details, please refer to our previous report.

2.3 MFC setup and operation

An H-shape dual chamber device was assembled as MFC reactor, and all MFCs were operated in batch mode with external resistance of 1000 Ω at 37 ℃. Cylindrical MFC chambers have a volume of 100 mL and separated by CMI7000 cation exchange membranes. An anode with a size of 1 × 1 cm connected with a titanium wire was

positioned in a cylindrical chamber of the MFC, with a carbon brush (3 × 5, diameter × length) as a cathode placed in the opposite chamber. For MFC start-up, the anode chamber was inoculated with 10 mL pre-acclimated bacteria from another well-running MFC, 10 mL anaerobic sludge solution and 80 mL fresh anolyte, and the cathode chamber was filled with 100 mL of 50 mM potassium ferricyanide and 50 mM potassium chloride. When the operating voltage dropped below 50 mV, both anodic and cathodic fluids were renewed.

The output voltage was recorded every 10 min using a data acquisition system (PS2024V, Smacq, China). After several cycles of stable voltage output, the polarization and power density curves were obtained by tuning the circuit resister from 5000 to 100 Ω. Both the current density and power density were normalized to the total anode surface area (2.0 cm^2). Coulombic efficiency (η) was calculated according to Eq. (2):

$$\eta = C_{output}/C_{total} \times 100\% \quad (2)$$

Where, C_{output} is the total coulombs calculated by integrating the current over time for a complete circle, in Coulombs; and C_{total} is the total theoretical amount of charge (Q, in Coulombs) transferred in the acetate oxidation process [S3].

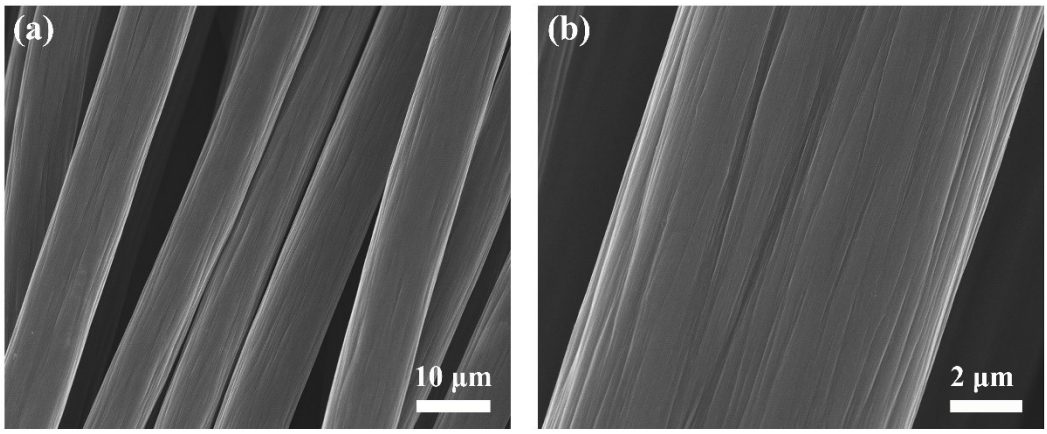

Fig. S1 Low magnification (a) and high magnification (b) SEM images of CC.

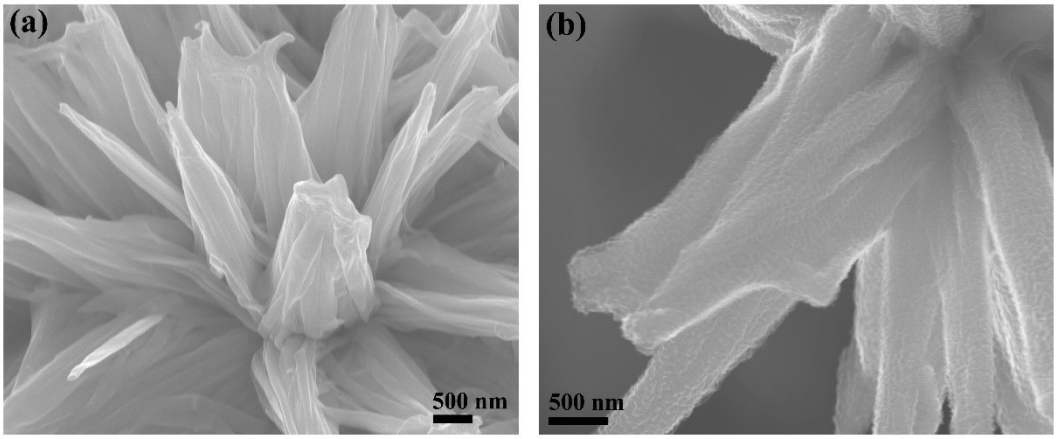

Fig. S2 High magnification SEM images of MoC-CC (a) and MoC@PANI-CC (b).

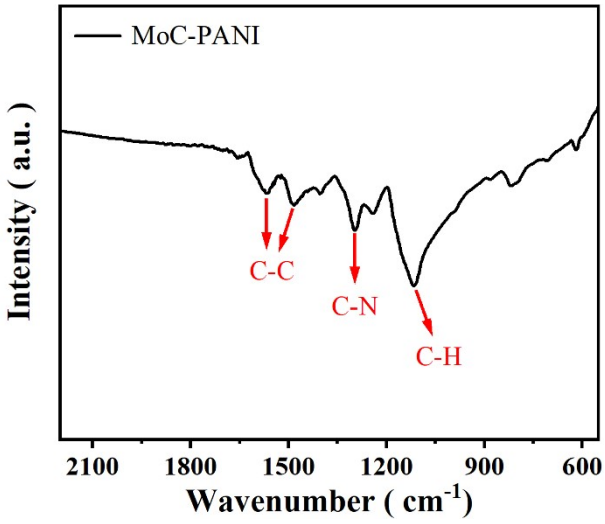

Fig. S3 FTIR spectra of MoC-PANI

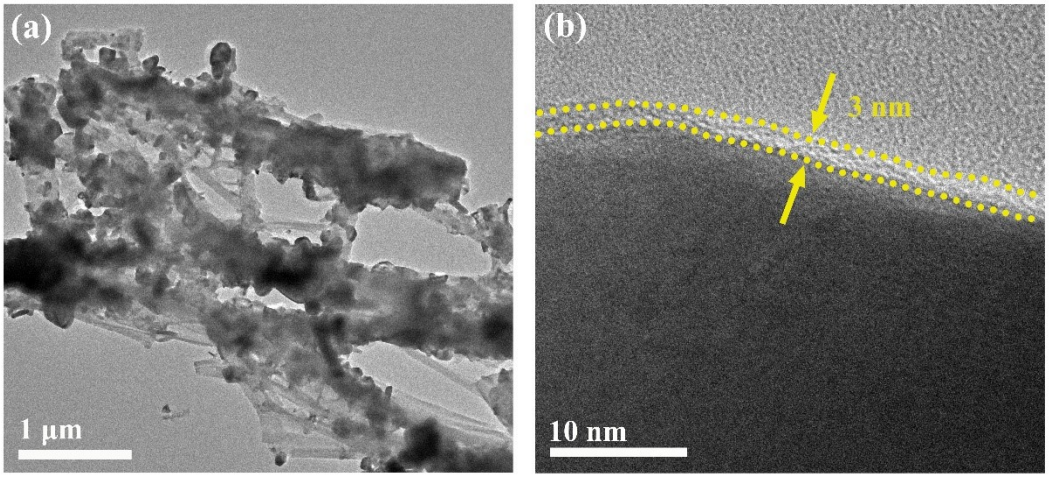

Fig. S4 TEM (a) and HRTEM (b) images of MoO_2/MoC@NC

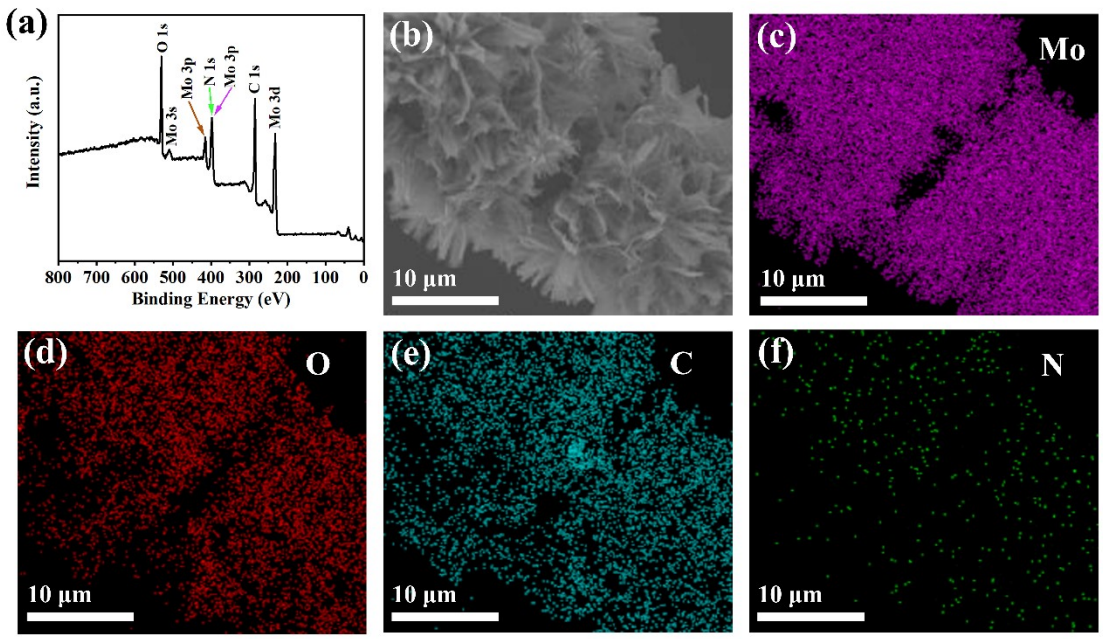

Fig. S5 XPS full spectrum of MoO_2/MoC@NC-CC (a). SEM image of MoO_2/MoC@NC-CC (b) and the corresponding elemental mapping images of this material for Mo (c), O (d), C (e) and N (f), respectively.

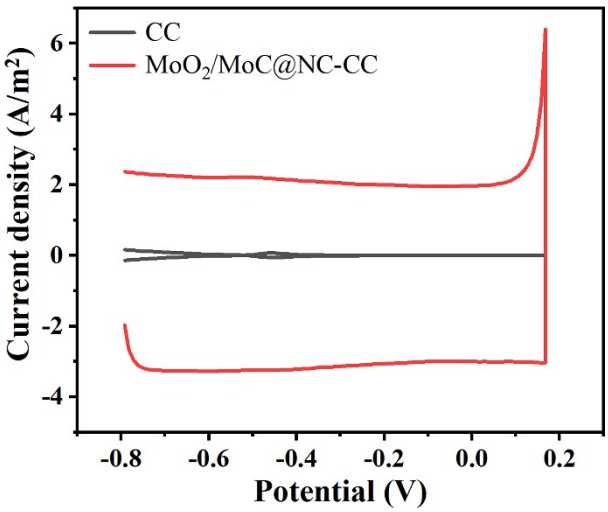

Fig. S6 DPV of both anodes without biofilms in fresh anolyte

Table S1. Performance comparison of MFC with anodes modified different Mo-based nanomaterials

Anode	Maximum Power density (W/m^2)	Microorganism	Feed	Configure	Ref
Mo_2C/CCT	1.12	mixture	acetate	Single-chamber	[S4]
8.31 wt% Mo_2C@CF	1.025	*S. putrefaciens* CN32	lactate	Dual-chamber	[S5]
16.7 wt% Mo_2C/CNT	1.05 ± 0.0264	*E. coli*	glucose	Single-chamber	[S6]
Mo_2C@G	1.697	*S. putrefaciens* CN32	lactate	Dual-chamber	[S7]
Mo_2C/CF	0.27	*K. pneumoniae* strain L17	glucose	Single-chamber	[S8]
Mo_2C/RGO	1.747 ± 0.038	*E. coli* k12	glucose	Dual-chamber	[S9]
MoO_2/PANI (1:2 w/w)	1.101	mixture	glucose	Single-chamber	[S10]
GL-MoS_2-CC	0.96	mixture	acetate	Dual-chamber	[S11]
Ni_3Mo_3C/CF	0.25	*K. pneumoniae* strain L17	glucose	Dual-chamber	[S12]
Co-MoO_2/NCND/CF	2.06 ± 0.05	mixture	acetate	Single-chamber	[S13]
MoO_2/MoC@NC-CC	2.93	mixture	acetate	Dual-chamber	This work

References

[S1] X. Zhang, F. Zhou, W. Pan, Y. Liang and R. Wang, Advanced Functional Materials 2018, 28, 1804600. DOI: 10.1002/adfm.201804600

[S2] K. Devarayan, D. Lei, H. Y. Kim and B. S. Kim, *Chemical Engineering Journal*, 2015, 273, 603-609. DOI: 10.1016/j.cej.2015.03.115

[S3] L. Zhuang, S. Zhou, Y. Li, and Y. Yuan, *Bioresour Technol*, 2010, 101, 3514-9. DOI: 10.1016/j.biortech.2009.12.105

[S4] L. Zeng, S. Zhao, L. Zhang, and M. He, *RSC Advances*, 2018, 8, 40490-40497. DOI: 10.1039/c8ra07502f

[S5] L. Zou, Z. Lu, Y. Huang, Z.E. Long, and Y. Qiao, *Journal of Power Sources*, 2017, 359, 549-555. DOI: 10.1016/j.jpowsour.2017.05.101

[S6] Y. Wang, B. Li, D. Cui, X. Xiang, and W. Li, *Biosens Bioelectron*, 2014, 51, 349-55. DOI: 10.1016/j.bios.2013.07.069

[S7] L. Zou, Y. Huang, X. Wu and Z.-e. Long, *Journal of Power Sources*, 2019, 413, 174-181. DOI: 10.1016/j.jpowsour.2018.12.041

[S8] L. Zeng, L. Zhang, W. Li, S. Zhao, J. Lei and Z. Zhou, *Biosens Bioelectron*, 2010, 25, 2696-700. DOI: 10.1016/j.bios.2010.05.002

[S9] W. Guo, M. Chen, X. Liu, F. Cheng and X. Lu, *Chemistry*, 2021, 27, 4291-4296. DOI: 10.1002/chem.202005020

[S10] Geetanjali, R. Rani and S. Kumar, *International Journal of Hydrogen Energy*, 2019, 44, 16933-16943. DOI:

10.1016/j.ijhydene.2019.04.201

[S11] X. Lou, Z. Liu, J. Hou, Y. Zhou, W. Chen, X. Xing, Y. Li, Q. Liao and X. Zhu, *Catalysis Today*, 2021, 364, 111-117. DOI: 10.1016/j.cattod.2019.11.029

[S12] L. Z. Zeng, S. F. Zhao and W. S. Li, *Appl Biochem Biotechnol*, 2015, 175, 2637-46. DOI: 10.1007/s12010-014-1458-1

[S13] X. Li, M. Hu, L. Zeng, J. Xiong, B. Tang, Z. Hu, L. Xing, Q. Huang and W. Li, *Biosens Bioelectron*, 2019, 145, 111727. DOI: 10.1016/j.bios.2019.111727